

The effect of Selected Cement Brands in Kenya on the Critical Penetration Depth of Rust in Reinforced Concrete Water Conveyancing Structures

Philip Mogire^{1,a,*}, Silvester Abuodha^{2,b}, John Mwero^{3,c} and Geoffrey Mang'uriu^{4,d}

^{1,2,3}Department of Civil and Construction Engineering,
University of Nairobi, Kenya

⁴Department of Civil, Construction and Environmental Engineering,
Jomo Kenyatta University of Agriculture & Technology
P.O. Box 62000-00200, Nairobi, KENYA

^aphilosiemo@yahoo.com, ^bsochieng@yahoo.com, ^cjohnmwero1@gmail.com, ^dgmanguriu@yahoo.co.uk

DOI: 10.29322/IJSRP.8.11.2018.p8333

<http://dx.doi.org/10.29322/IJSRP.8.11.2018.p8333>

Abstract- As the world economies shift to support the United Nations sustainable development goals, new cement manufactures have entered into the Kenyan market producing brands of ordinary Portland Cement meeting the minimum requirement of the Kenya Bureau of Standards. The variant parameter in this brands is the chemical composition of the cement Brands. The aim of this research was to establish the relationship between the cement Brand and the Critical penetration depth of rust and their role in the durability of the reinforced concrete structures.

To achieve the desired objective three cement brands out of six brands manufactured in Kenya; CemX, CemY and Cem Z of ordinary Portland cement with compressive strength 42.5N/mm^2 were sourced from a wholesaler for the study. Other concrete constituent materials; fine and coarse aggregates and steel were obtained from the local Kenyan market. This research was conducted at the University of Nairobi Structures/ Concrete laboratory and the State Department of Infrastructure in the Ministry of Transport, Infrastructure, Housing and Urban Development of the Government of Kenya.

The physical and chemical properties of the materials were investigated for compliance to relevant applicable British and Kenyan standards and if they met the acceptable criteria. Concrete of characteristic strength of 25N/mm^2 derived from the DOE method was used. Concrete materials were batched by weight and mixed by a lab electric pan concrete mixer in batches of 0.009 m^3 . The concrete batches were tested for consistency by the slump and compaction factor tests. For each brand of cement 9 cubes of $150\text{mm} \times 150\text{mm} \times 150\text{mm}$ for compression test, 9 cylinders of $150\text{mm} \times 300\text{mm}$ for tensile strength and 9 cylinders of $150\text{mm} \times 300\text{mm}$ for accelerated corrosion test were cast. After 24 hours the cast specimens were demolded and immersed in curing tanks for 27 days.

Specimens for compression and tensile test were tested at 7, 14 and 28 days while the specimens for accelerated corrosion were immersed in a 3.5% industrial sodium chloride solution under 6V. The accelerated corrosion specimens were monitored for onset of cracks and stopped when the cracks were 0.1mm in width. From the results in the research, the different Kenyan selected cement brands linearly correlate with the critical penetration depth of rust and the rate of corrosion for the evolution of 0.1mm crack width and this is attributed to their chemical composition.

Index Terms- Cement Brands, accelerated corrosion test, Critical penetration depth of Rust.

1. INTRODUCTION

For the medium term (2018-2022) of vision 2030, the Republic of Kenya defined four items referred to The Big Four Agenda aimed at accelerating economic growth, focusing on manufacturing, food security and nutrition, and providing universal health coverage and affordable housing. The big four agenda is anchored in Vision 2030 of Kenya and form a commitment in achieving part of the 17 UN Sustainable Development Goals of Vision 2030 for a better and sustainable world. Reinforced concrete Water conveyancing structures play a significant role in the Big Four Agenda and defining the service life is crucial in Kenya's economic sustainability.

Steel is thermodynamically unstable under normal atmospheric conditions and will release energy and revert back to its natural state of iron oxide(rust) and this process is called corrosion. For corrosion to occur in reinforced concrete; the rebar must be at different energy levels, the concrete must act as an electrolyte, and the rebar must act as a metallic connection.

At high pH (12- 13) reinforced concrete is in an alkaline state and thin oxide layer forms on the steel and prevents metal atoms from dissolving forming a passive film [1]. This passive film reduces the corrosion rate to an insignificant level without which the steel would corrode at rates at least 1,000 times higher [2]

Corrosion in reinforced concrete has a significant effect in the service life of structures and is caused by electrochemical reactions with contaminants. The presence of rust on reinforcement bars and appearance of cracks parallel to the reinforcement bars symbolize the presence of corrosion in reinforced concrete. Carbonation inducing a generalized attack and the presence of chlorides inducing a localized attack are the main causes of electrochemical corrosion in reinforced concrete as shown in Figure 1[2].

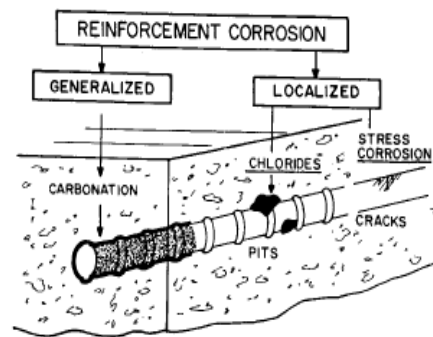
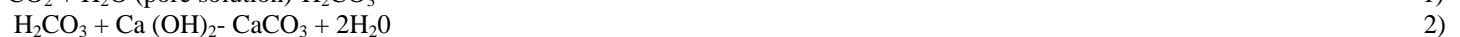


Figure 1: Types and morphology of the corrosion in concrete: generalized (carbonation), localized (chlorides)[2]

Carbonation

In this process atmospheric carbon dioxide diffuses to the steel concrete interface and reacts with the calcium and alkaline hydroxides and cement as shown in equation 1 and 2, lowering the pore solution pH value at the rebar concrete interface to below 9 thus initiating corrosion.



Carbonation does not occur if the concrete is water-saturated or in very dry conditions because moisture is required to form carbonic acid which attacks the Ca(OH)_2 and diffusion of CO_2 through water is very slow. Carbonation is very slow and generally follows the square root time law shown in equation 3.

$$x = K\text{CO}_2 t^{0.5} \quad 3)$$

Where

x = carbonation depth after time t

$K(\text{CO}_2)$ = carbonation coefficient/factor for a given concrete

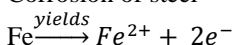
Chloride attack

The chloride ions may be present in the concrete originating from its constituent materials but the most common source is from outside due to the structure being in an aggressive environment with chloride ion species. Surface chlorides diffuses to the rebar concrete interface and induces local disruption of steel passive layer through the reactions of equation 4 -6 leading into formation of pits on the reinforcement bars.

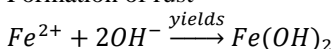
Decomposition of the passivity layer



Corrosion of steel



Formation of rust



The electrochemical reactions take place in the limited volume of aqueous solution present in the pores of the concrete and steel interface. This process results in loss of mass and cross sectional area of steel resulting in reduced load carrying capacity and structural failure. The internal stresses generated by rust which is of a lower density and thus bulkier than the parent steel leads to formation of cover cracking to account for more space required to accommodate the rust. Other effects include reduction of steel-concrete interface bond stains on the concrete surface, delamination and spalling. Previous studies, using various analytical and microscopy techniques,

have shown that corrosion products forms in the cement paste adjacent to a corroding rebar [e.g. 3, 4, 5, 6, 7]. The corrosion products continually get deposited at the steel and concrete interface generating stresses that cause progressive deterioration [8]. Chlorides ingress through the net of pores is one of the most common reasons that cause corrosion in reinforcements when these are located in an aggressive environment or when in the mixture such ions are incorporated. Chloride ions are capable of causing localized corrosion therefore leading to a premature and unexpected failure of the structures [9].

2. CHLORIDE PENETRATION INTO CONCRETE

In water conveyancing reinforced concrete structures chloride ions are either bound, adsorbed or dissolved in water that is retained in the pores, which forms the pore solution. The total chlorides (combined free and bound) content do not give a realistic indication of the risk of corrosion to the reinforcement but an assessment of the long-term risk to structures exposed to chlorides.

Chlorides from the aggressive external environment penetrate into the interconnected pores or capillary pores, as well as micro and macro-cracks in concrete by convection and the chloride ions diffuse further into the saturated pore system. The concentration gradients of the free chlorides control the process of diffusion. Chloride ions that are harmful to the reinforcing steel are those which are dissolved or are free, but due to the balances that occur, it is possible that chloride ions which are adsorbed, be incorporated into the solution and become hazardous [10][11].

When free chloride ions penetrate the pore system of the concrete structure, some of the ions are fixed to solid concrete structure. The transient chemical reaction affects the flow of free ions in the pore solution. Considering a water conveyancing structure as submerged, the primary chloride transport mechanism is diffusion. The critical penetration depth of rust is shown in figure 2.

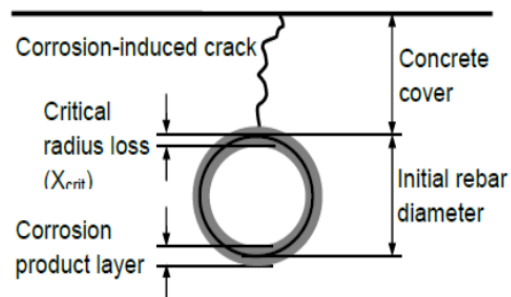


Figure 2: Critical penetration depth of rust of critical radius loss X_{crit} [12]

3.0 METHODOLOGY

This research was conducted at the University of Nairobi Structures/ Concrete laboratory where the physical properties of the materials, sample preparation and testing were done. The chemical properties of the materials were done at State Department of Infrastructure in the Ministry of Transport, Infrastructure, Housing and Urban Development of the Government of Kenya.

3.1 Concrete samples

In the constituent materials for test samples, three series of specimens were prepared with a variation in the selected brand of cement; cement brand X, Y, Z of Ordinary Portland cement (42.5N/mm²), all commercially available in Kenya and manufactured in accordance to KS EAS 18-1: 2001[13], an adoption of the European Norm EN 197 cement standards. Other materials used were, clean river sand, and 20mm maximum size coarse aggregate potable water and 10mm reinforcement bar.

3.1.1 Cement

The chemical composition of each brand of cement used was tested in accordance with KS EAS 18-1: 2001. Three Brands of Cement used in the research were sourced from one wholesaler for three different manufacturers. The cement brands used are denoted CemX, CemY and CemZ in the subsequent parts of this research.

3.1.2. Reinforcement bars

Reinforcing ribbed steel bars used had a tensile strength of strength 500N/mm² cut to length and sourced from a local manufacturer. The reinforcing ribbed steel bars were 27 pieces of 10mm diameter and 400 mm long with 120mm wire brushed to remove the mill scale and sprayed with zinc coat in the Lab. The bars were kept in the lab covered with a dry cloth and kept free of moisture until just before concrete placement. Any visible corrosion product was removed by wire brushing prior to placing the bars in the moulds during casting. A single bar was placed at the geometrical centre of the moulds with 120 mm protruding from the concrete cast surface as shown in figure 3.1

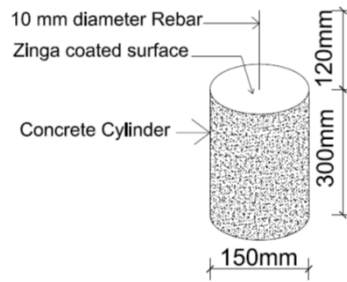


Figure 3.1 Detail of embedded ribbed bar in concrete

3.1.3 Other concrete materials

Table 1 shows description and source of other materials of concrete used in the research.

Table 3.1. Details of materials used in the research

SN	Description	Source	Remark
1.	Fine aggregates	Stockpile vender sourced from Machakos River	This was washed and oven dried before use.
2.	Coarse aggregates	Kenya builders quarry	5-20mm quarry graded
3.	Mixing water	Tap water in the Lab	

3.2. Experimentation

3.2.1. Concrete Composition

A mix was designed to meet the requirements of strength, water-cement ratio and cement content for concrete water conveyancing structures. The target strength was 25N/mm². The concrete was batched by weights using the building research establishment (BRE) mix design concrete mix. The mix design is shown in Table 3.2.

Table 3.2 Basic mix design

Material	Coarse aggregates	Fine aggregates	Ordinary Portland Cement	Total Free water
Quantity	1300 kg/m ³	650kg/m ³	450 kg/m ³	450 litres/m ³

Nine specimens per cement brand were cast in a cylindrical mould, 300mm long and 150mm diameter. After casting, the specimens were kept in laboratory conditions (23 °C) for 24 hours. Subsequently, the specimens were de-moulded and stored in a curing tank for 27 days.

3.2.2 Exposure

After curing the test specimens were dried for 24 hours in laboratory conditions and then subjected to accelerated corrosion in a tank containing 3.5 % NaCl at room temperature as shown in figure 3.2.



Figure 3.2 Samples of the concrete cylinders in accelerated corrosion set up.

3.2.3 Open circuit potential measurements (OCP)

Monitoring of the electrochemical potential was performed by immersing a stainless steel electrode as the anode and in the sodium chloride solution and each group of specimens arranged in series in the cathode as shown in figure 3.3. During the experiment the cathodic and anodic current was measured with time and any crack evolution and size monitored. The experiment in each series was stopped when the biggest crack size reached 0.1mm. During the duration of the test, no replacement of the sodium chloride solution was performed.

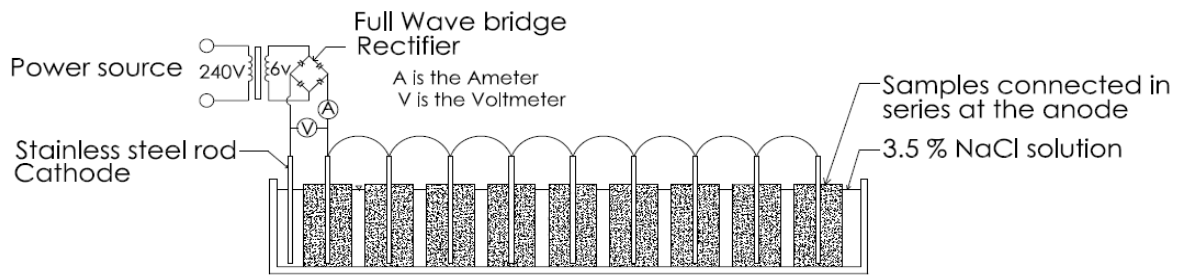


Figure 3.3 Sketch of experimental circuit set up

3.3.4 Detection of the onset of corrosion-induced Cracking

Once the specimens were subjected to anodic polarization, the applied current and voltage were monitored on a daily, then weekly basis until corrosion induced cracking appeared on the concrete surface. A detailed optical examination utilizing a graduated optical ruler and lens with 100X-magnification was done on a biweekly basis. The optical examination was required to check for invisible cracks and to accurately measure crack width.

3.3.5 Estimation of critical penetration depth of rust (X_{crit})

The cracked specimens were demolished to retrieve the reinforcing steel segments for inspection of corrosion morphology and for gravimetric evaluation of mass (see figure 3.4). The extent to which the steel corrosion product was radially transported into surrounding concrete were visually examined. The surface area of corroded carbon steel regions was estimated by the area covered by the steel corrosion product which were confirmed after rust removal.



Figure 3.4 Images of corrosion samples after corrosion.

The steel corrosion product was removed off the surface of reinforcement bar segments in accordance with the procedure of ASTM G1-03 [ASTMG01-2003]. The measured amount of lost steel mass in grams was estimated by subtracting the final weight measured after cleaning from the initial weight. The theoretical mass loss in grams of steel resulting from the applied current was calculated based on Faraday's first law of electrolysis.

$$\Delta m_F = [M \times I \times t / (n \times F)] \quad 7)$$

where $(M/n \times F)$ is the electrochemical equivalence of the iron substance

M is the molar mass of iron ($M=55.847$ g/mol),

n is the effective valence of the iron ions dissolving ($n=2$) and

F is Faraday's constant ($F=96485$ C/mol).

I is the applied anodic current in amperes

t is the time in seconds during which the current has been passed through the circuit.

$$\text{Current Efficiency} = \Delta m_G / \Delta m_F \quad 8)$$

The distribution of corrosion along and around the perimeter of carbon steel segments was examined and detailed images taken. The surface of the reinforcement bars was partially corroded therefore the average value of X_{crit} was estimated by:

$$X_{cr_{eq}} / \mu m = \frac{\Delta m \cdot 10^4}{\rho \cdot A} \quad 9)$$

Where ρ is the density of carbon steel (7.858 g/cc)

A is the surface area of the corroded length of the rebar in mm^2

Δm is the change in mass of reinforcement bars in grams

Rate of corrosion in mm/year

Corrosion Rate= $87.6 \times [w / (D \times A \times T)]$

10)

where W is the weight loss in milligrams,

D is the density of the material used in g/cc

A is the area of the specimen (cm²), and

T is the duration of the test period in hours.

4.0 RESULTS AND DISCUSSION.

4.1.1 Results of Chemical composition of the brands of cement tested.

The chemical composition in table 4.1 is given in terms of oxides except for the insoluble residue (IR) and Loss of Ignition(LOI).

Table 4.1 Result of Chemical composition the brands of cement tested.

SN	Test	Result			KS EAS 18-1: 2001 Requirement
		Cem X	CemY	Cem Z	
1.	CaO%	59.86	59.11	58.82	Sum \geq 50
2.	SiO ₂ %	16.56	21.56	19.47	
3.	SO ₃ %	2.02	2.78	2.03	\leq 3.5
4.	MgO%	1.76	1.04	0.57	\leq 5
5.	K ₂ O%	0.027	0.051	-	
6.	Fe ₂ O ₃ %	2.32	3.48	1.44	
7.	Al ₂ O ₃	7.61	8.09	6.85	3-8
8.	Na ₂ O ₃ %	0.054	0.018		
9.	LOI%	0.11	0.10	4.75	\leq 5
10.	Cl%	0.012	0.016	0.014	\leq 0.1
11.	IR%	2.20	0.55	1.96	\leq 5

4.1.2 Effect of Chemical Composition of Cement Samples on the rate of corrosion.

The different brands however had varying properties attributed to their manufacturing processes and manufacturer.

Some constituent compounds in the cement brands are of varying amounts and are responsible in differences exhibited in the resultant concrete properties.

a) Effect of Lime (CaO) and silicon dioxide (SiO₂) on the critical penetration depth of rust and the rate of corrosion

From table 4.1 there is a notable variation in the amounts of CaO, SiO₂ and Insoluble Residue. CemX has the highest amount of CaO (59.86%), CemY has the highest SiO₂ (21.56%) and CemX has the highest Insoluble residue (2.20%). Both CaO and SiO₂ increases the compressive strength of concrete though SiO₂ has to be limited relative to CaO in order not to negatively affect setting time. The optimum amount of nano-SiO₂ is still unknown because of the fact that the SiO₂ used in different studies are of different types with different particle size, specific surface area and associated production method[14]. In addition, uniform dispersion of SiO₂ in cementitious materials is another issue. The effect of SiO₂ include acting as a filler, nucleation and improving the microstructure and early age compressive strength of the cement. Higher compressive strength depicts a concrete with a more compact matrix and a low ingress rate of chloride ions for the chloride induced corrosion mechanism and hence cement with a higher amount of lime and silicon dioxide will have a smaller critical penetration depth of rust and a low rate of corrosion.

b) Effect of CaO/SiO₂ on the critical penetration depth of rust and the rate of corrosion

The ratio of lime (CaO) to silicon dioxide (SiO₂) contents in ordinary Portland cement should be greater than 2. The restriction on the ratio of lime to silicon dioxide [14] is to ensure that the quantity of silicon dioxide is considerably lower than that of lime so that the setting of concrete is not inhibited and the higher ratio increase the compressive strength and a smaller critical penetration depth of rust and lower corrosion is expected. The lime-silicon dioxide ratio for cement samples X, Y, and Z were 3.61, 2.71 and 3.0 respectively.

c) Effect of SO₃ on the critical penetration depth of rust and the rate of corrosion

The amount of SO₃ in all the cement brands were within the acceptable limit. SO₃ controls the setting time of cement to avoid flash set. Kosmatka et al, (1991). Slower setting results in greater compressive strength to the set mass and smaller critical penetration depth and slower rate of corrosion.

c) Effect of MgO on the critical penetration depth of rust and the rate of corrosion

The quantity of magnesium oxide (MgO) in ordinary Portland cement should not exceed 5% [10]. All the cement samples satisfied this requirement with 1.76%, 1.04% and 0.57% for cement samples X, Y and Z respectively. Magnesium oxide contributes to the colour of cement and hardness of the resulting concrete. If the quantity of MgO is in excess of 5 percent, cracks will appear in concrete and which may affect the rate of corrosion by generating spots for penetration of chloride ions in concrete.

d) Effect of Chloride Content on the critical penetration depth of rust and the rate of corrosion

The chloride content in ordinary Portland cement should be less than 0.4%. All the cement samples in this work satisfied this requirement. Higher amounts of chloride in the cements will contribute to the bound chloride and subsequently to the total amount available for electrochemical reactions in corrosion due to chloride mechanism and subsequently increase the critical penetration depth and the rate of corrosion.

e). Effect of Al₂O₃ Content on the critical penetration depth of rust and the rate of corrosion

The quantity of aluminum oxide in all the brands was within the acceptable limits. An increase in the Al₂O₃ results in an increase in the time for the initial and final sets and hence an increase in compressive strength resulting in a smaller critical penetration depth and a lower rate of corrosion.

4.2 Aggregates

4.2.1 Properties of aggregates

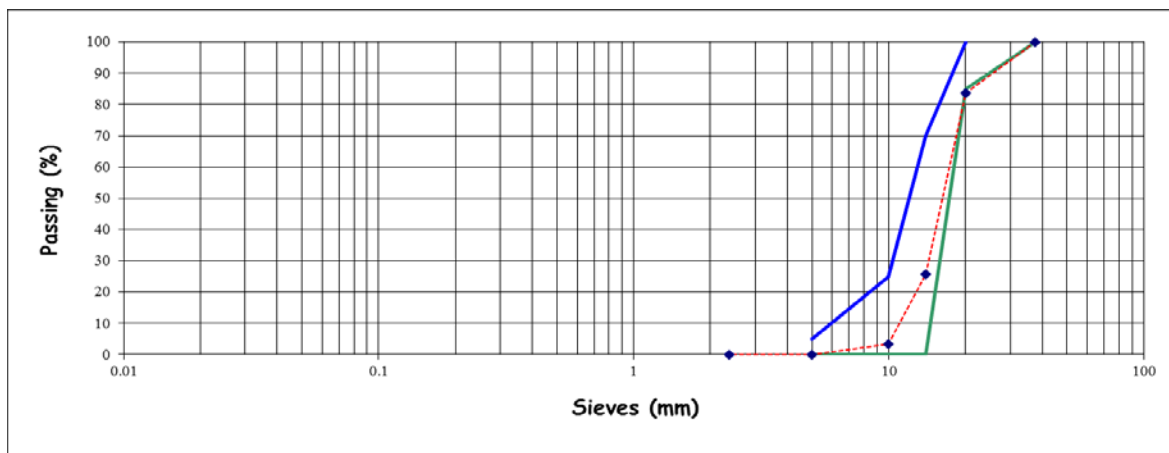
Various tests were carried out on the aggregates to determine their suitability for the research. Water soluble chlorides ions percent were found to be zero in fine aggregates, 0.002 % in coarse aggregates all less than 0.03% acceptable in compliance with BS EN 12620: 2002. Table 4.2 and Table 4.3 show the physical and mechanical properties of the aggregates used while graph 4.1 and graph 4.2 show the gradation of the aggregates.

Table 4.2: Physical properties of aggregates used in the study

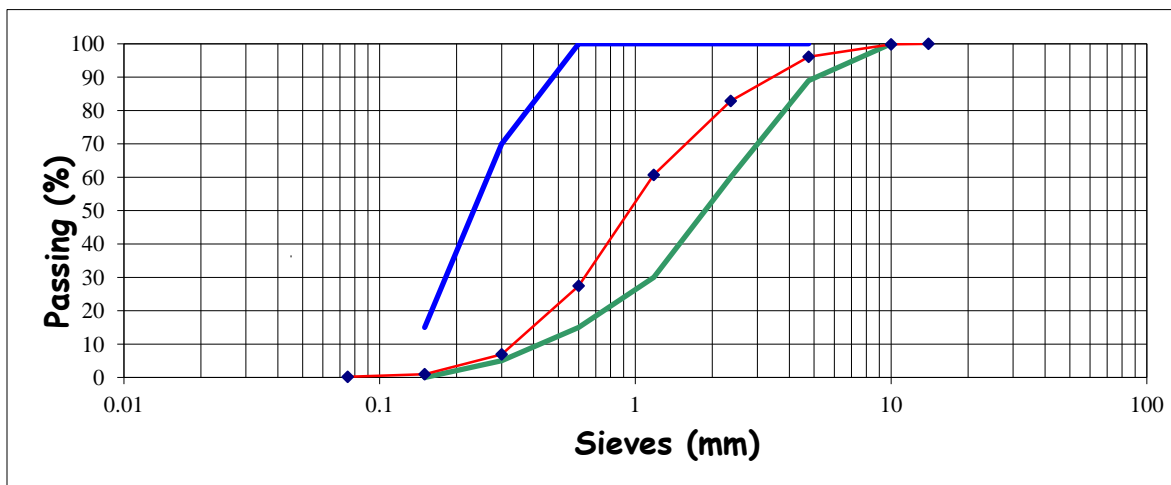
Material	Specific gravity	Absorption %	Silt content %	Max Size
Fine aggregates	2.6	1.8	7.4	4.0
Coarse aggregates	2.6	0.3	0	20.0

Table 4.3: Mechanical properties carried on coarse aggregates.

Test	Size of aggregates mm	Crushing value %	Impact Value %	Flakiness index %	Loss Angeles Abrasion Value %
Result	5-20	18	8	35	20



Graph 4.1 Gradation of Coarse aggregates



Graph4.2: Gradation of fine aggregates

4.2.1 Effect of Properties of aggregates on critical penetration depth of rust and the rate of corrosion

The physical properties, mechanical properties and gradation of aggregates directly affect the compressive strength and fracture energy. Table 4.2 and 4.3 show the physical and mechanical properties of the materials used. Figure 4.1 and 4.2 show the gradation of the aggregates as well graded which results in a compact matrix of the resulting concrete and subsequently an influence in the critical penetration depth of rust and the rate of corrosion. In this research there was no variation in the aggregates used.

4.3 Hardened properties of concrete

Table 4.4 shows the compressive strength of the brands of cement used.

Table 4.4 Results of Average Compressive strength with time

SN	Cement Brand	Compressive Strength in N/mm ²		
		7days	14 days	28 days
1.	CemX	25.81	40.28	41.29
2.	CemY	36.379	39.23	44.89
3.	CemZ	34.81	36.26	41.09

4.3.2 Effect of hardened properties of concrete on the critical radius loss and the rate of corrosion

From the results of table 4.4, the compressive strength of the concrete reduced with use of cement brand Y, X and Z respectively. This effectively affectively reduces the rate of ingress of chloride ions and the critical penetration depth of rust the rate of corrosion.

4.4 Accelerated corrosion

Table 4.5 shows the result of accelerated corrosion while table 4.6 shows the relationship between compressive strength, critical penetration depth of rust and the rate of corrosion.

Table 4.5 Measurement of Electrode current with time

Brand of Cement	CemX	CemY	CemZ
Date Cast	30.09.2017	02.10.2017	03.2010.2017
Start of accelerated corrosion	29.10.2017	31.10.2017	01.11.1717
Current at Immersion	Anode	290mA	150mA
	Cathode	269mA	140mA
Current after 30 days	Anode	269mA	140mA
	Cathode	240mA	140mA
Current at 0.1mm crack	Anode	90mA	95mA
	Cathode	98mA	98mA
Duration of crack of 0.1mm	109 days	115 days	106 days
$\Delta m [(M \times I \times t)/(n \times F)]$,	246 grams	274grams	226 grams
Δm_{actual}	1.06grams	0.649grams	1.15grams
Average surface area	1100mm ²	786 mm ²	1162mm ²

corroded,(A)			
Theoretical Critical radius loss Xcrit.	28mm	44mm	25mm
Actual Critical radius loss Xcrit.	0.12mm	0.105mm	0.13mm
Rate of corrosion mm/yr	0.41	0.36	0.43

Table 4.6 Relationship between the compressive strength, actual critical radius loss and the rate of corrosion

SN	Cement Brand	Compressive Strength in N/mm ²			Actual critical radius loss(mm)	Rate of Corrosion(mm/yr)
		7days	14 days	28 days		
1.	Cem X	25.81	40.28	41.29	0.12	0.41
2.	Cem Y	36.379	39.23	44.89	0.105	0.36
3.	Cem Z	34.81	36.26	41.09	0.13	0.43

From tables 4.5 and 4.6 the following can be noted that samples with the highest compressive strength, took the longest period for a crack of 0.1mm to be reached in accelerated corrosion, the lowest critical penetration radius and rate of corrosion and the converse is also true. This results also confirm the trend expected from the chemical compounds in the Cem X, Cem Y and Cem Z. In higher compressive strengths the capillary pore spaces are smaller and successfully reduce the rate of ingress of surface chloride to the rebar/concrete interface. Thus, the diffusion of chloride ions will drop sharply with increased strength and exposure time reducing the critical penetration depth and the rate of corrosion.

5. CONCLUSION

This research investigated the effect of selected cement brands in Kenya on the critical penetration depth of rust and the rate of corrosion. The chemical composition of the brands of cement show a marked variation in chemical composition whose effect in compression strength linearly correlate with the critical penetration depth of rust and the rate of corrosion. From the results, for achieving a crack width of 0.1mm in the same accelerated corrosion setup, there is a linear variation in the critical penetration depth of rust and the rate of corrosion for the selected brand of cement.

REFERENCES

- [1] P.Ghods, O.B. Isgor, F. Bensebaa, D. Kingston, "Angle-resolved XPS study of carbon steel passivity and chloride-induced depassivation in simulated concrete pore solution," *Corros. Sci.* 2012, 58, 159-167.
- [2] ACI Committee 222, "Protection of Metals in Concrete Against Corrosion," ACI 222R-01, American Concrete Institute, Farmington Hills, Michigan, 2001.
- [3] A.K. Aligizaki, M.R. de Rooij, D.D. Macdonald, "Analysis of iron oxides accumulating at the interface between aggregates and cement paste," *Cem. Concr. Res.*, 30 (2000) 1941-1945.
- [4] G.S. Duffó, W. Morris, I. Raspini, C. Saragovi, "A study of steel rebars embedded in concrete during 65 years," *Corros. Sci.*, 46 (2004) 2143-2157.
- [5] O. Poupard, V.L'Hostis, S. Catinaud, I. Petre-Lazar, "Corrosion damage prognosis of a reinforced concrete beam after 40 years natural exposure in marine environment," *Cem. Concr. Res.*, 36 (2006) 504-520.
- [6] T.D. Marcotte, C.M. Hansson, "Corrosion products that form on steel within cement paste," *Mater Struct.*, 40 (2007) 325-340.
- [7] S. Caré, Q.T. Nguyen, V. L'Hostis, Y. Berthaud, "Mechanical properties of the rust layer induced by impressed current method in reinforced mortar," *Cem. Concr. Res.*, 38 (2008) 1079-1091.
- [8] F.P. Glasser, K.K. Sagoe-Crentsil, "Steel in concrete: Part II Electron microscopy analysis," *Mag. Concr. Res.*, 41 (1989) 213-220.
- [9] W. Aperador, R. Mejía de Gutiérrez, D.M. Bastidas, "Steel corrosion behaviour in carbonated alkali-activated slag concrete," *Corrosion Science*, vol.51, 2009.
- [10] W. Aperador, R. Vera, A.M. Carvajal, "Evaluation of the cathodic protection applied to steel embedded in the ASS using the finite element method" *International Journal of Electrochemical Science*, 7(2012)12870. 5
- [11] E. Busba and A. Sagüés, "Critical Localized Corrosion Penetration of Steel Reinforcement for Concrete Cover Cracking," NACE International's Annual Conference and Exposition, CORROSION, 201
- [12] R. Montoya, W. Aperador, D.M. Bastidas, "Steel corrosion behaviour in carbonated alkali-activated slag concrete," *Corrosion Science*, 51(2009)2857
- [13] Kenya Bureau of Standards, *KS EAS 18-1:2001-Cement Part 1:Composition, Specification and Conformity Criteria for Common Cements*. Kenya Bureau of Standards, Nairobi, 2005.
- [14] BS 12, "Specification for Portland cement," BSI Publications, London, 1996.

AUTHORS

First Author – Mogire Philip, PhD Student, Department of Civil and Construction Engineering, University of Nairobi, Kenya, philosiemo@yahoo.com

Second Author – Prof. Silvester Abuodha, Associate Professor, Department of Civil and Construction Engineering,

University of Nairobi, Kenya, sochieng@yahoo.com

Third Author – Dr. John Mwero, Lecturer, Department of Civil and Construction Engineering, University of Nairobi, Kenya, johnmwero1@gmail.com.

Fourth Author – Prof. Geoffrey Mang'uriu, Professor, Department of Civil, Construction and Environmental Engineering, Jomo Kenyatta University of Agriculture & Technology, gmanguriu@yahoo.co.uk

Correspondence Author – Mogire Philip, philosiemo@yahoo.com, +254 734 967 989